Available online at www.sciencedirect.com
SCIENCE DIRECT®
Earth and Planetary Science Letters 232 (2005) 287–294
EPSL
www.elsevier.com/locate/epsl

Spinel in Martian meteorite SaU 008: Implications for Martian magnetism

Yongjae Yu*, Jeff S. Gee

Scripps Institution of Oceanography, La Jolla, CA 92093-0220, USA

Received 3 September 2004; received in revised form 9 December 2004; accepted 9 December 2004
Available online 5 March 2005
Editor: V. Courtillot

Abstract

Shergotty–Nakhla–Chassigny (SNC) meteorites provide the only available samples of Martian material. The stable permanent magnetization of SNC meteorites has been traditionally attributed to magnetite (Fe_3O_4) or pyrrhotite (Fe_7S_8). On the basis of rock magnetic, microscopic, and electron microprobe analyses on rock chips and mineral separates, we suggest that a new material (Fe–Cr–Ti spinel) is responsible for the stable paleomagnetic record of Martian meteorite SaU 008. It is possible that SaU 008 acquired a primary remanence of thermal origin from the Martian crustal field. However, this proposition requires further testing because the effect of shock events on Fe–Cr–Ti spinel is unknown.

Keywords: Mars; spinel; SNC meteorites; SaU 008; magnetism

1. Introduction

Mars currently possesses no magnetic field of internal origin. The estimated maximal present-day Martian magnetic field originating from weak Martian dipole is ~0.5 nT at the equator, compared to ~30,000 nT for Earth [1]. However, strong surface magnetizations have been inferred from high amplitude magnetic anomalies over much of the southern hemisphere [2,3]. Very low surface magnetizations in the younger northern hemisphere indicate that the crust was formed after the cessation of the Martian dynamo [2–4] or that the crust has been demagnetized [5]. Since the southern hemisphere is older, it has been suggested that younger andesitic volcanism resurfaced most of the northern lowlands [6] or the basalts in northern hemisphere have been weathered [7]. High amplitude magnetic anomalies are confined mostly to the older southern terrains, implying that the Martian magnetic field existed only during the early Noachian (~4 Ga). However, the exact timing of initiation/cessation of the Martian dynamo is still unresolved [8,9]. Furthermore, a recent analysis of the Mars Orbiter laser Altimeter (MOLA) data suggests that the Martian lowlands (in northern hemisphere) are older than the plains that cover them [10].

* Corresponding author.
E-mail address: yjyu@ucsd.edu (Y. Yu).

0012-821X/$ - see front matter © 2004 Elsevier B.V. All rights reserved.
doi:10.1016/j.epsl.2004.12.015

Martian meteorites can potentially provide information on the timing and the magnitude of the Martian dynamo. There are about two dozen Shergoty–Nakhla–Chassigny (SNC) meteorites, whose Martian origin has been confirmed by isotopic measurements of trapped noble gases in shock-melted glass [11]. For instance, the estimated CO_2 and N_2 in SNC meteorites is in agreement with that determined by mass spectrometer measurements made by the Viking Lander [12]. The crystallization age of SNCs varies from 165 Ma to 4.51 Ga, but they all show young ejection ages <20 Ma [11]. SNCs typically contain maskelynite shock metamorphosed plagioclase), pyroxene, olivine, and opaque minerals (mostly chromites).

Earlier paleomagnetic investigations on SNC meteorites suggested that at least part of the natural remanent magnetization (NRM) of SNCs was possibly acquired in an ambient magnetic field on the parent body [13–23]. Interpretation of the origin of the remanence in SNC meteorites, however, is complicated by uncertainty in the magnetic phase responsible for the stable remanence. For example, Fe-sulfide and (titano)magnetite have both been suggested as the dominant remanence carriers in ALH 84001 [17–19,22,23]. In addition, Weiss et al. [22] noted a weak magnetic signal apparently associated with Cr-spinels ($Fe_{1.05}Cr_{1.31}Al_{0.35}Mg_{0.20}Ti_{0.06}O_4$). However, two most recent studies all indicate that magnetite (whether biogeneic or shock-produced from iron-rich carbonate) is the main remannece carriers in ALH 84001 [22,23].

2. Martian meteorite SaU 008

A total of 9923 g of SaU 005/008 was retrieved on 26 November, 1999 at Sayh al Uhaymir desert, Oman.

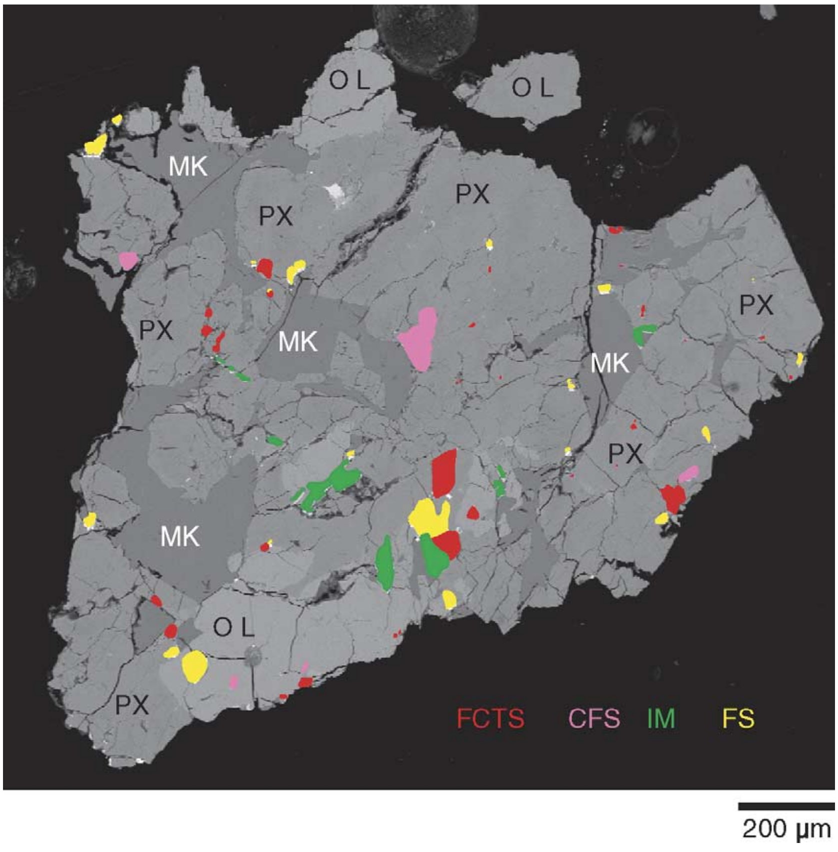

Fig. 1. SEM image of the thin section of SaU 008 showing abundant Olivine (OL), Pyroxene (PX), and Maskelynite (MK). Four opaque minerals are Cr–Fe spinel (CFS), Fe–Cr–Ti spinel (FCTS), ilmenite (IM), and Fe-sulfide (FS).

Two main pieces of SaU 005/008 (combined 9923 g) were collected at two sites (which are ~2 km apart) on Sayh al Uhaymir Desert, Oman. Other additional fragments are SaU 051 (436 g), SaU 060 (42 g), SaU 090 (95 g), SaU 094 (223 g), SaU 120 (75 g), and SaU 150 (107 g) [24]. In this study, we report magnetic data from a shergottite meteorite SaU 008, a Martian meteorite collected in the Sayh al Uhaymir desert of Oman [24], which suggests a new type of material (Fe–Cr–Ti spinel) as the dominant magnetic remanence carrier.

SaU 008 drew attention because it shows the least terrestrial weathering among SNCs and because it was crystallized in a plutonic regime [24]. In particular, lack of zonation and bigger size of groundmass strongly indicates that SaU was crystallized at plutonic or sub-volcanic environment [24]. The radiometric and ejection ages of a sister meteorite SaU 005 are 1.01±0.11 Ga [25] and 1.27–1.50 Ma [25,26]. Mineralogic data from a sister meteorite SaU 094 showed three main minerals ~48–58% pyroxene (dominantly pigeonite), ~22–31% olivine (Fo_{65-69}) and ~8–16% plagioclase together with minor amounts of chromite, titanian magnesium chromite, ilmenite, and pyrrhotite [24,27,28].

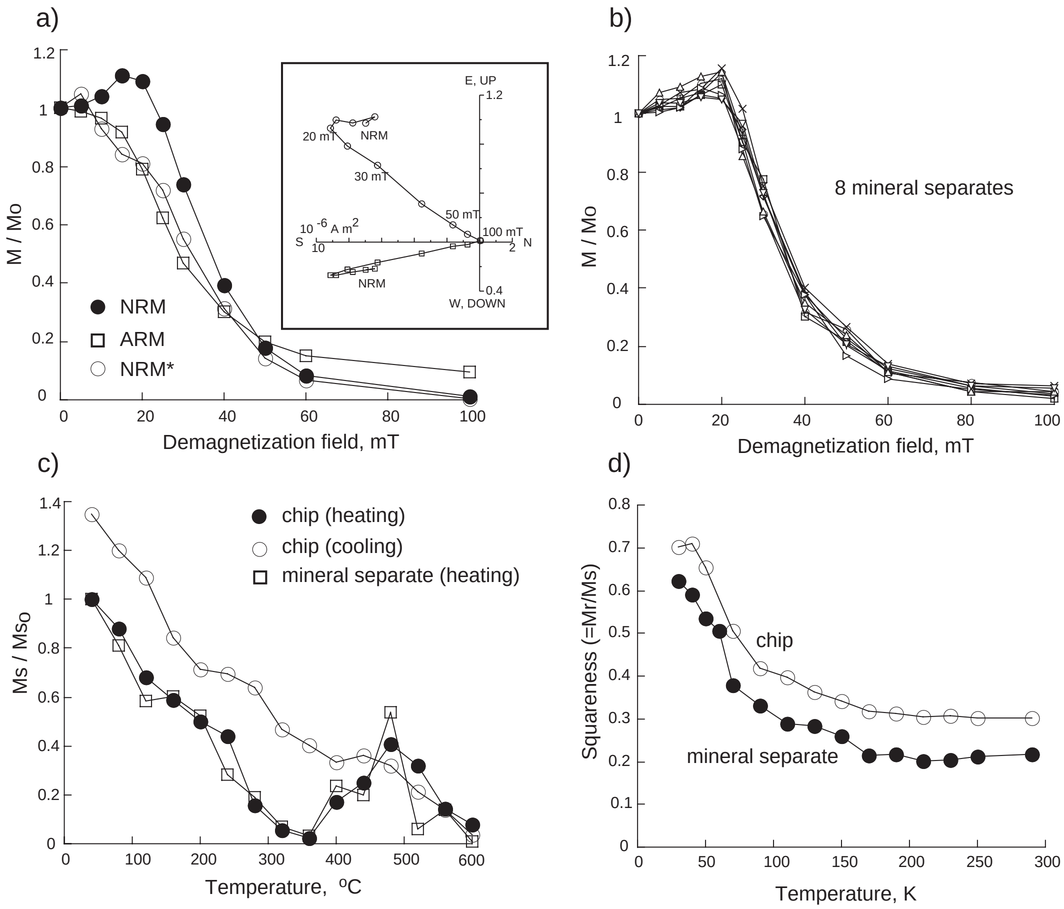

Fig. 2. a) Alternating-field (AF) demagnetization of anhysteretic remanence (ARM) and natural remanence (NRM). Inset is the vector projection of AF demagnetization of NRM in which open circles and squares represent horizontal- and vertical-plane projections. NRM* is calculated by projecting the overprinted fraction (AF demagnetization from 0 to 20 mT) towards the direction of primary remanence. Note that ARM and NRM* show similar AF demagnetization spectra. b) A similar demagnetization trend of NRM was observed for the bulk chip (see a)) and 8 mineral separates. c) Temperature dependence of saturation magnetization (=M_s) at high temperatures. d) Variation of squareness (=saturation remanence over saturation magnetization, M_r/M_s) as a function of temperatures.

3. Results

In this study, we used three mm size chips and 20 individual opaque separates of SaU 008. Scanning electron microscopy (SEM) identified olivine, abundant pyroxene (pigeonite), maskelynite, and other opaque phases (Fig. 1).

Stepwise alternating-field (AF) demagnetization was carried out using a Sapphire Instruments SI-4 static AF generator. AF demagnetization indicates that SaU 008 has a stable remanence with two magnetization components (Fig. 2a). A low stability component, representing about 15% of the NRM, was removed by AF demagnetization to 20 mT (Fig. 2a,b). AF demagnetization of NRM* and anhysteretic remanent magnetization (ARM) is very similar (Fig. 2a). NRM* is calculated by projecting the overprinted fraction (AF demagnetization from 0 to 20 mT) towards the direction of primary remanence. ARM was generated in an AF decaying from 180 mT with a superimposed steady field of 100 μT. In vector projection (see inset of Fig. 2a), the characteristic component spans AF demagnetization from 20 to 100 mT. Thermal demagnetization was not carried out because the temperature dependence of magnetic hysteresis (measured on a sister chip) indicated that significant alteration began at 350 °C (Fig. 2c).

What mineral is responsible for this stable magnetic component? Four opaque minerals were identified from SEM and electron microprobe analyses: Fe-sulfide, ilmenite, and two spinels (Fig. 1, Tables 1 and 2). For microscopic analysis, we used FEI Quanta 600 Environmental SEM and Cameca Camebax micro-beam electron microprobe facility at the Scripps Institution of Oceanography. For SEM work, opaque minerals were compositionally homogeneous in multiple analyses ~2 μm spot size.

Table 2
Composition of Fe-sulfide (bulk chip) based on electron microprobe analysis

Element	Fe-sulfide (%)	Normalized to S
Al	0.14	0.0046
Ca	0.02	0.0002
Cr	0.05	0.0008
Fe	58.30	0.9313
Mg	0.62	0.0219
Mn	0.04	0.0002
Ni	4.90	0.0755
S	34.76	1
Si	1.20	0.0371
Ti	0.03	0.0006
Total	99.47	

All the reported values are the average of 10 microprobe analyses.

Both spinels are rich in Cr, Fe, and Ti and have significant amounts of Al and Mg (Table 1). We term these spinels Cr–Fe spinel ($Cr_{1.53}Fe_{0.84}Al_{0.29}Mg_{0.23}Ti_{0.06}O_4$) and Fe–Cr–Ti spinel ($Fe_{1.44}Cr_{0.63}Ti_{0.45}Mg_{0.23}Al_{0.23}O_4$). Of the four opaque phases, ilmenite is paramagnetic and therefore will not contribute to the room-temperature remanence. We observed no hematite (Fe_2O_3), either as discrete grains or as lamellae within ilmenite. The absence of hematite or hematite–ilmenite lamellae in SNCs is common,

Table 1
Composition of oxides (bulk chip and magnetic separates) based on electron microprobe analysis

Wt.%	Cr–Fe spinel	Fe–Cr–Ti spinel	3 magnetic separates	Ilmenite
# of determination	5	6	6	5
Al_2O_3	7.06 (2.08)	5.61 (1.06)	4.92 (1.60)	1.29 (2.17)
CaO	0.12 (0.11)	0.10 (0.07)	0.01 (0.02)	0.07 (0.09)
Cr_2O_3	55.10 (4.11)	22.49 (2.73)	20.37 (3.74)	0.61 (0.53)
$FeO+Fe_2O_3$	27.60 (3.47)	48.74 (3.95)	49.95 (2.43)	42.95 (3.52)
MgO	4.44 (0.90)	4.30 (0.45)	3.54 (1.22)	5.02 (2.28)
MnO	0.02 (0.02)	0.02 (0.04)	0.01 (0.02)	–
NiO_2	0.10 (0.14)	0.02 (0.03)	0.01 (0.02)	–
SiO_2	1.08 (1.44)	0.55 (0.25)	0.04 (0.04)	0.80 (0.77)
TiO_2	2.23 (4.97)	16.99 (3.76)	20.29 (3.11)	48.79 (1.45)
Total	99.11	98.82	99.15	99.53

All the reported values are the average of several electron microprobe analyses. Numbers within the bracket represent the difference between maximum and minimum weight percentage. Sulfur was absent on these oxides.

Table 3
Composition of oxides (non-magnetic mineral separates) based on electron microprobe analysis

Wt.%	Mineral separate A	Mineral separate B
# of determination	2	2
Al_2O_3	5.98	0.60
CaO	0.45	0.07
Cr_2O_3	56.09	0.80
$FeO+Fe_2O_3$	29.09	44.44
MgO	4.32	4.90
MnO	0.00	0.00
NiO_2	0.13	0.00
SiO_2	0.05	0.61
TiO_2	2.38	48.39
Total	98.49	99.81

All the reported values are the average of two electron microprobe analyses. Mineral separate A and B are Cr–Fe spinel and ilmenite, respectively (see Table 1).

despite the emphasis placed on these phases as a potential source of strong magnetic anomalies on Mars (e.g., [29–33]).

As commonly observed in other SNCs, SaU 008 also contains Fe-sulfide (Fig. 1). Electron microprobe data indicate compositions (Fe/S~0.93, Table 2) between that of antiferromagnetic (non-magnetic) troilite (FeS) and hexagonal pyrrhotite ($Fe_{10}S_{11}$), rather than ferrimagnetic monoclinic pyrrhotite (Fe_7S_8). The lack of a low-temperature transition at 30–34 K during magnetic hysteresis measurements also confirms that the monoclinic form (Fe_7S_8) of magnetic pyrrhotite is absent in SaU 008 (Fig. 2d). Thus, it appears that either the Cr–Fe spinel or Fe–Cr–Ti spinel (Table 1) may be responsible for the remanence in SaU 008.

In order to clarify the magnetic phase responsible for the stable NRM behavior, we compared the magnetic behavior of rock chips with that of individual mineral separates. Among 20 individual mineral separates (60–200 μm in length) that we analyzed, 12 grains were too weakly magnetized to measure ($<5\times10^{-8}$ A m^2) while 8 grains had a measurable remanence and show demagnetization behavior of NRM that closely matches that of the rock chips (Fig. 2b).

We have also determined the temperature dependence of hysteresis using a low-temperature vibrating sample magnetometer at the Institute for Rock Magnetism, University of Minnesota. Hysteresis loops were measured at various temperatures from 30 K to 290 K in a peak field of 1 T in field increments of 10 mT. The similarity between rock chips and mineral separates is also found in the temperature dependence of magnetic hysteresis (Fig. 2c,d). For example, both chips and individual separates show essentially the same variation during heating (Fig. 2c). The substantial alteration above 300 °C precludes the estimation of the Curie temperature, but the Curie point must be above 300 °C (Fig. 2c). The squareness (defined as saturation remanence (M_r) over saturation magnetization (M_s)) shows a systematic broad increase below 150 K (Fig. 2d). Grain size differences of the remanence carriers can explain the slight difference of squareness between magnetic separates and the host chips (Fig. 2d). In particular, the small Fe–Cr–Ti spinels embedded within silicates (Fig. 1) may result in a higher squareness for the rock chips (Fig. 2d).

Most importantly, electron microprobe data indicate that all analyzed magnetic separates that show similar magnetic behaviors to the host chips are Fe–Cr–Ti spinels (Table 1). They have compositions very similar to the Fe–Cr–Ti spinels observed inside the host chip (Fig. 1, Table 1). Thus, the Fe–Cr–Ti spinel grains apparently are responsible for the stable magnetic record of SaU 008. In order to explain the magnitude of the NRM of the host chip, we need 1.1–1.6% volume concentration of magnetic Fe–Cr–Ti spinel (e.g., 108.2–136.3 mA/m for magnetic separates versus 1.50–1.71 mA/m for rock chips). This

Table 4
Composition of Fe-sulfide (non-magnetic mineral separates) based on electron microprobe analysis

Element	Fe-sulfide (%)	Normalized to S
Al	0.03	0.0010
Ca	0.01	0.0002
Cr	0.00	0.0000
Fe	58.24	0.9533
Mg	0.01	0.0004
Mn	0.01	0.0002
Ni	5.65	0.0883
S	34.97	1
Si	0.15	0.0049
Ti	0.03	0.0006
Total	99.10	

The reported values are the average of 4 microprobe analyses.

estimation roughly fits with the observed amount of Fe–Cr–Ti spinel under the SEM photo (Fig. 1).

Among 20 individual mineral separates that we analyzed, 12 grains were too weakly magnetized to measure (<5×10^{-8} A m^2). In order to exclude the possibility that other phases are responsible for the magnetic remanence, we carried out electron microprobe analysis on non-magnetic separates. We observed Cr–Fe spinel, ilmenite, and sulfide (Tables 3 and 4) whose compositions are virtually identical to those observed within the bulk chip (Tables 1 and 2). Thus, we can safely dismiss the possibility that Cr–Fe spinel, ilmenite, and sulfide are contributing to the magnetic remanence.

4. Discussions

While the observed data suggest that the Fe–Cr–Ti spinel is responsible for the remanence in SaU 008, little is known about the magnetic properties of intermediate composition in the spinel solid solution series. Of the end member spinel compositions, only Fe_3O_4 and $MgFe_2O_4$ are magnetic at room temperature with spontaneous magnetizations of 480 kA/m [34] and 112 kA/m [35], respectively. Since most of other spinel end member compositions are non-magnetic at room temperature, a linear mixing model might suggest a spontaneous magnetization of the Fe–Cr–Ti spinel ($Fe_{1.44}Cr_{0.63}Ti_{0.45}Mg_{0.23}Al_{0.23}O_4$) that is ~20–30% of that of Fe_3O_4. The observed spontaneous magnetization of $Fe_{1.44}Cr_{0.63}Ti_{0.45}Mg_{0.23}Al_{0.23}O_4$ was 148–162 kA/m, roughly fits with the estimation. Although we cannot exclude fine scale exsolution of other magnetic phases (such as Fe_3O_4 and $MgFe_2O_4$), even complete exsolution of such phases appears inadequate to account for the observed high spontaneous magnetization.

The observed Fe–Cr–Ti spinel ($Fe_{1.44}Cr_{0.63}Ti_{0.45}Mg_{0.23}Al_{0.23}O_4$) contains abundant Ti, somewhat different with the composition of magnetic Fe–Cr rich spinel often observed on terrestrial rocks (e.g., [36–38]). It is possible that the terrestrial Cr/Fe-rich spinel involves a simple solid-solution of two end members (magnetite and chromite) while the Martian Cr/Fe-rich spinel involves additional contribution from other end members such as ulvospineal ($Fe_2^{2+}TiO_4$) and/or Mg_2TiO_4.

Similar AF demagnetization of the NRM and ARM (Fig. 2a) may imply a thermal origin of the NRM because ARM and TRM share similar AF demagnetization spectra [39]. If the remanence is a TRM, does SaU 008 provide a record of the Martian magnetic field? Given the age (~1.0 Ga), the remanence might reflect either a field of internal origin for a long-lived dynamo [8,9] or a remanence produced by the Martian crustal field generated by an early dynamo [2–4].

The results above highlight several difficulties with using meteorite samples to make inferences about the Martian dynamo. First, most previous magnetic studies have lacked definitive information (electron microprobe data) on the composition of the opaque phases and/or the low-temperature analyses [13–23]. As shown in recent studies ([24], this study), the observed Fe-sulfide is often not magnetic. Furthermore, lingering uncertainties in the remanence carriers for ALH 84001 have led to varying interpretations of the significance of the remanence in this ancient meteorite [17–19,22,23].

Second, the possible role of impact events in modifying the remanence carried by pyrrhotite [20,40] and Fe-oxide [41–45] has recently been emphasized. There are at least two shock events (Martian ejection and terrestrial entrance) that could influence the magnetization of SNCs. In particular, the Martian ejection phase is often accompanied by pressures of over 15 GPa and temperatures over a few hundred degrees Celsius [11]. For example, (U–Th)/He thermochlonology suggests that SNC meteorite Los Angeles experienced a strong shock during ejection [46]. On the other hand, U–Th–Pb dating on ALH 84001 phosphates show no evidence of extended heating since 4 Ga [47].

If NRM is affected by shock events, can paleomagnetism resolve such a signal? Unfortunately, a standard zero-field demagnetization alone is poorly suited to detect the effect of shock events. We suggest that paleointensity determination (although it is a destructive technique) would provide the most unambiguous evidence for shock events and the significance of the remaining primary remanence in meteorite samples such as ALH 84001. Because the ejection age of SNC meteorites are uniformly young (<20 Myr) [11] and occurred at a time where the Martian dynamo was likely absent [2–4], shock effects might be expected to demagnetize some fraction of the preexisting remanence. Then, it should produce a distinctive sigmoidal pattern of paired zero-field and in-field step heatings because the sample will acquire a laboratory remanence while maintaining nearly constant NRM for the temperature intervals that were affected during the shock events.

Regardless of whether SaU 008 preserves a record of the Martian field, Fe–Cr–Ti spinel should be considered as a candidate for explaining the high amplitude Martian magnetic anomalies and the stable remanence of SNCs. The Curie point for the Fe–Cr–Ti spinel is >300 °C, permitting remanence at depths of up to 20–60 km assuming a thermal gradient of 5–15 K/km [48].

Acknowledgements

John C. Bridges in the Natural History Museum, London, UK generously provided samples for use in this study. Helpful reviews by Mike Fuller and Ben Weiss improved the paper. We shared fruitful discussions with Lisa Tauxe. We wish to thank Evelyn York and Ray Fitzgerland of the facility lab, Scripps Institution of Oceanography for SEM and electron microprobe analyses. We thank Mike Jackson, Jim Marvin, and Peat Solheid of the Institute for Rock Magnetism (IRM) for their help with the measurements. The Keck foundation, the National Science Foundation, Earth Sciences Division, and the University of Minnesota provide funding for the IRM. This research was supported by NSF grant EAR0229498.

References

[1] M.H. Acuña, J.E.P. Connerney, P. Wasilewski, R.P. Lin, D. Mitchell, K.A. Anderson, C.W. Carlson, J. McFadden, H. Rene, C. Mazelle, D. Vignes, S.J. Bauer, P. Cloutier, N.F. Ness, Magnetic field of Mars: summary of results from the aerobraking and mapping orbits, J. Geophys. Res. 106 (E10) (2001) 23403–23417.

[2] M.H. Acuña, J.E.P. Connerney, N.F. Ness, R.P. Lin, D. Mitchell, C.W. Carlson, J. McFadden, K.A. Anderson, H. Reme, C. Mazelle, D. Vignes, P. Wasilewski, P. Cloutier, Global distribution of crustal magnetization discovered by the Mars Global Surveyor MAG/ER experiment, Science 284 (1999) 790–793.

[3] F. Nimmo, D.J. Stevenson, Influence of early plate tectonics on the thermal evolution and magnetic field of Mars, J. Geophys. Res. 105 (E5) (2000) 11969–11979.

[4] J. Arkani-Hamed, An improved 50-degree spherical harmonic model of the magnetic field of Mars derived from both high-altitude and low-altitude data, J. Geophys. Res. 107 (E10) (2002) 5083.

[5] L.L. Hood, N.C. Richmond, E. Pierazzo, P. Rochette, Distribution of crustal magnetic fields on Mars: shock effects of basin-forming impacts, Geophys. Res. Lett. 30 (6) (2003) 1281.

[6] D. Rogers, P.R. Christensen, Age relationship of basaltic and andesitic surface compositions on Mars: analysis of high-resolution TES observations of the northern hemisphere, J. Geophys. Res. 108 (E4) (2003) 5030.

[7] M.B. Wyatt, V.E. Hamilton, H.Y. McSween Jr., P.R. Christensen, L.A. Taylor, Analysis of terrestrial and Martian volcanic compositions using thermal emission spectroscopy. 1: determination of mineralogy, chemistry, and classification stratigies, J. Geophys. Res. 106 (2001) 14711–14732.

[8] M. Purucker, D.T. Ravat, H.V. Frey, C.V. Voorhies, T. Sabaka, M.H. Acuña, An altitude-normalized magnetic map of Mars and its interpretation, Geophys. Res. Lett. 27 (2000) 2449–2452.

[9] G. Schubert, C.T. Russell, W.B. Moore, Timing of the Martian dynamo, Nature 408 (2000) 666–667.

[10] H.V. Frey, J.H. Roark, K.M. Shockey, E.L. Frey, S.E.H. Sakimoto, Ancient lowlands on Mars, Geophys. Res. Lett. 29 (10) (2002) 1384.

[11] L.E. Nyquist, D.D. Bogard, C.Y. Shih, A. Greshake, D. Stoffler, O. Eugster, Ages and geologic histories of Martian meteorites, Space Sci. Rev. 96 (2001) 105–164.

[12] R.O. Pepin, On the origin and evolution of terrestrial planet atmospheres and meteoritic volatiles, Icarus 92 (1991) 2–79.

[13] T.N. Nagata, Paleomagnetism of Antarctic achondrites, Mem. Natl. Inst. Polar Res., Spec. Issue 17 (1980) 233–242.

[14] S.M. Cisowski, Magnetic studies on Shergotty and other SNC meteorites, Geochim. Cosmochim. Acta 50 (1986) 1043–1948.

[15] D.W. Collinson, Magnetic properties of Antarctic shergottite meteorites EETA 79001 and ALHA 77005: possible relevance to a Martian magnetic field, Earth Planet. Sci. Lett. 77 (1986) 159–164.

[16] D.W. Collinson, Magnetic properties of Martian meteorites: implications for an ancient Martian magnetic field, Meteorit. Planet. Sci. 32 (1997) 803–811.

[17] J.L. Kirschvink, A.T. Maine, H. Vali, Paleomagnetic evidence of a low-temperature origin of carbonate in the Martian meteorite ALH84001, Science 275 (1997) 1629–1633.

[18] R.B. Hargraves, J.M. Knudsen, P. Bertelsen, W. Goetz, H.P. Gunnlaugsson, S.F. Hviid, M.B. Madsen, M. Olsen, Magnetic enhancement on the surface of Mars? J. Geophys. Res. 105 (E1) (2000) 1819–1827.

[19] B.P. Weiss, J.L. Kirschvink, F.J. Baudenbacher, H. Vali, N.T. Peters, F.A. Macdonald, J.P. Wikswo, A low temperature transfer of ALH84001 from Mars to Earth, Science 290 (2000) 791–795.

[20] P. Rochette, J.-P. Lorand, G. Fillion, V. Sautter, Pyrrhotite and the remanent magnetization on SNC meteorites: a changing perspective on Martian magnetism, Earth Planet. Sci. Lett. 190 (2001) 1–12.

[21] J. Shaw, M.J. Hill, S.J. Openshaw, Earth Planet. Sci. Lett. 190 (2001) 103–109.

[22] B.P. Weiss, H. Vali, F.J. Baudenbacher, J.L. Kirschvink, S.T. Stewart, D.L. Shuster, Earth Planet. Sci. Lett. 201 (2002) 449–463.

[23] M. Antretter, M. Fuller, E. Scott, M. Jackson, B. Moskowitz, P. Solheid, Paleomagnetic record of Martian meteorite ALH84001, J. Geophys. Res. 108 (E6) (2003) 5049.

[24] E. Gnos, B. Hofmann, I.A. Franchi, A. Al-Kathiri, M. Hauser, L. Moser, Sayh al Uhaymir 094: anew Martian meteorite from the Oman desert, Meteorit. Planet. Sci. 37 (2002) 835–854.

[25] J. Park, K. Nagao, R. Bartoschewitz, Noble gas studies on Sayh al Uhaymir 150 Martian meteorite, Ann. Meteorol. Soc. Meet. 67 (2004) 5129.

[26] M. Paetsch, M. Altmaier, U. Herpers, H. Kosuch, R. Michel, L. Schultz, Exposure age of the new SNC meteorite Sayh al Uhaymir 005, Meteorit. Planet. Sci. 35 (2000) A124–A125.

[27] J. Zipfel, Sayh al Uhaymir 005/008 and its relationship to Dar al Gani 476/489, Meteorit. Planet. Sci. 35 (2000) A178.

[28] R. Bartoschewitz, P. Appel, Sayh al Uhaymir 150: a further fragment of the SaU-Shergottite shower, Meteorit. Planet. Sci. 38 (2003) A38.

[29] G. Kletetschka, P.J. Wasilewski, P.T. Taylor, Unique thermoremanent magnetization of multidomain hematite: implications for magnetic anomalies, Earth Planet. Sci. Lett. 176 (2000) 469–479.

[30] D.J. Dunlop, G. Kletetschka, Multidomain hematite: source of planetary magnetic anomalies? Geophys. Res. Lett. 28 (2001) 3345–3348.

[31] S.A. McEnroe, R.J. Harrison, P. Robinson, F. Langhorst, Nanoscale hematite–ilmenite lamellae in massive ilmenite rock: an example of 'Lamellar Magnetism' with implications for planetary magnetic anomalies, Geophys. J. Int. 151 (2002) 890–912.

[32] Ö. Özdemir, D.J. Dunlop, Thermoremanence and stable memory of single-domain hematites, Geophys. Res. Lett. 29 (2002) 1877.

[33] P. Robinson, R.J. Harrison, S.A. McEnroe, R.B. Hargraves, Lamellar magnetism in the hematite–ilmenite series as an explanation for strong remanent magnetization, Nature 418 (2002) 517–520.

[34] S. Akimoto, Magnetic properties of FeO–Fe_2O_3–TiO_2 system as a basis of rock magnetism, J. Phys. Soc. Jpn. 17B (1962) 706–710.

[35] H.S.C. O'Neill, H. Annersten, D. Virgo, The temperature dependence of the cation distribution in magnesioferrite ($MgFe_2O_4$) from powder XRD structural refinements and Mossbauer spectroscopy, Am. Mineral. 77 (1992) 725–740.

[36] A. Kumar, M.S. Bhalla, Sources of stable remanence in chromite ores, Geophys. Res. Lett. 11 (1984) 177–180.

[37] M.W. Hounslow, Ferromagnetic Cr and Mn spinels in sediments: residual magnetic minerals after diagenetic dissolution, Geophys. Res. Lett. 23 (1996) 2823–2826.

[38] Y. Yu, D.J. Dunlop, O. Ozdemir, H. Ueno, Magnetic properties of Kurokami pumices from Mt. Sakurajima, Japan, Earth Planet. Sci. Lett. 192 (2001) 439–446.

[39] Y. Yu, D.J. Dunlop, Ö. Özdemir, Are ARM and TRM analogs? Thellier analysis of ARM and pseudo-Thellier analysis of TRM, Earth Planet. Sci. Lett. 205 (2003) 325–336.

[40] P. Rochette, G. Fillion, R. Ballou, F. Brunet, B. Ouladdiaf, L. Hood, High pressure magnetic transition in pyrrhotite and impact demagnetization on Mars, Geophys. Res. Lett. 30 (13) (2003) 1683.

[41] J. Pohl, U. Bleil, U. Hornemann, Shock magnetization and demagnetization of basalt by transient stress up to 10 kbar, Z. Geophys. 41 (1975) 23–41.

[42] S.M. Cisowski, M. Fuller, The effect of shock on the magnetism of terrestrial rocks, J. Geophys. Res. 83 (B7) (1978) 3441–3458.

[43] S.A. Gilder, M. LeGoff, J. Peyronneau, J.-C. Chervin, Novel high pressure magnetic measurements with application to magnetite, Geophys. Res. Lett. 29 (10) (2002) 1392.

[44] S.A. Gilder, M. LeGoff, J.-C. Chervin, J. Peyronneau, Magnetic properties of single and multi-domain magnetite under pressures from 0 to 6 GPa, Geophys. Res. Lett. 31 (2002) L10612.

[45] G. Kletetschka, P.J. Wasilewski, Low-level shock in magnetite, titanohematite, and hematite, EOS Trans. AGU 83 (19) (2002) P41A-08.

[46] K. Min, P.W. Reiners, S. Nicolescu, J.P. Greenwood, Age and temperature of chock metamorphism of Martian meteorite Los Angeles from (U–Th)/He thermochronometry, Geology 32 (2004) 677–680.

[47] K. Terada, T. Monde, Y. Sano, Ion microprobe U–Th–Pb dating of phosphates in Martian Meteorite ALH 84001, Meteorit. Planet. Sci. 38 (2003) 1697–1703.

[48] L.L. Hood, A. Zakharian, Mapping and modeling of magnetic anomalies in the northern polar region of Mars, J. Geophys. Res. 106 (E7) (2001) 14601–14619.